

Assessing Indoor Environments with sUAS through Real-Time Virtual Reality and Assured Navigation

Maarten Uijt de Haag, Jessie Robinson, Adam Schultz, and Joel Huff, *Ohio University*

BIOGRAPHIES

Jessie Robinson is a B.S.E.E. student and Adam Schultz and Joel Huff are M.S.E.E. students within the School of Electrical Engineering and Computer Science at Ohio University. All three students are Research Associates with the Avionics Engineering Center and work on navigation and collision avoidance systems for small Unmanned Aircraft Systems (sUAS) in challenging environments.

Maarten Uijt de Haag is the Edmund K. Cheng Professor of Electrical Engineering at Ohio University and a Principal Investigator with the Ohio University Avionics Engineering Center. He earned his Ph.D. from Ohio University and holds an M.S.E.E. from Delft University of Technology, located in the Netherlands. He is a member of the ION, a Senior Member of the IEEE and an Associate Fellow of the AIAA. Dr. Uijt de Haag was the recipient of the Institute of Navigation Thurlow Award in 2007.

ABSTRACT

This paper discusses a method that uses a small-size unmanned aircraft system (sUAS) to navigate a challenging environment and generate, in real-time, a three-dimensional (3D) map (e.g., point cloud data of features) of that environment. The 3D map is then transmitted to a remote user and shown in raw or processed form in near real-time on a virtual reality (VR) headset for user interaction, scene interpretation and assessment. Furthermore, the paper will include flight test results of our multi-copter sUAS operating in both indoor and outdoor environments. In addition to these discussions, the paper will show some navigation and mapping performance results.

1. INTRODUCTION

The number of potential commercial applications for sUAS is increasing every day, especially at lower altitudes. Example applications include environmental monitoring, infrastructure inspection and maintenance, surveillance, mapping, agriculture, aerial photography, search and rescue, law enforcement. Some of these applications require the sUAS user to assess the environment observed by the sUAS (e.g., damage assessment, victim localization,

and threat assessment). In particular, multi-copter platforms have emerged as effective platforms for lower-altitude operations and could be very capable for cost-effective missions in remote or difficult locations. These environments are typically challenging in terms of obstacles that must be avoided, trajectories that must be planned and available navigation capabilities. The increased complexity of these environments furthermore drives the requirement for increased autonomy as manual decisions on navigation, collision avoidance and mission planning are too slow. In previous work, we developed a reliable navigation and mapping method for both outdoor and indoor structured environments that uses multiple platform laser scanners, an inertial measurement unit, barometric height and (where available) GNSS [1]. The method in [1] is based on a combination of a multiple laser-based Simultaneous Localization and Mapping (SLAM) solution, tight integrated navigation of dead-reckoning and GPS and an advanced altitude estimator, and will form the basis for the approach proposed in this paper. The method described in this paper performs several tasks simultaneously:

- (i) Use real-time GPS/IMU/laser/vision-based navigation method for autonomous navigation in a structured but challenging outdoor/indoor environment via a set of waypoints that can be planned by the user in real-time,
- (ii) Perform the necessary obstacle detection and avoidance when necessary,
- (iii) Use the pose (i.e., position and attitude) estimates to reference the laser-range scanner (and vision) measurements and generate a point-cloud representation of the environment,
- (iv) Transmit this data to a local ground station,
- (v) Show a raw or processed version of the observed environment in near real-time on a virtual reality (VR) headset for user interaction, scene interpretation and assessment.

Figure 1 shows an example challenging environment where the proposed navigation and mapping technology would be applied.



Figure 1. Example navigation and mapping environment.

In challenging environments such as the one shown in Figure 1, measurements from global navigation satellite systems, GNSS (e.g., GPS, Galileo, GLONASS, Beidou), are often unavailable or only sparsely available. Furthermore, if available, the measurement performance may be deteriorated due to multipath or the lack of direct line-of-sight (i.e., only measurements based on reflected signals are available). To alleviate the deteriorated GNSS performance (e.g., accuracy, availability, and continuity), alternative navigation methods must be used to assure that certain required navigation performance characteristics are met (i.e., accuracy, availability, continuity). Papers [2] and [3] provide various categories of alternative navigation: (a) integration of laser scanners and/or imagery with an inertial sensor, (b) the use of signals of opportunity, (c) and beacon-based navigation (e.g., pseudolites, UWB).

In this paper, the navigation and mapping methods are based on measurements from laser range scanners and monochrome cameras. The literature on using laser range scanners for both localization and simultaneous location and mapping is extensive. For example, in [4][5] the authors describe a method to use a 2D laser range scanner integrated with an inertial installed on an sUAS to navigate in a structured environment. Rather than using a 2D laser range scanner, [6] described an integrated navigation example using 3D imagers. Both methods address integrity aspects of the navigation solution as well. While both these methods focus on navigation alone others have addressed the simultaneous estimation of pose and a map of the environment (i.e., SLAM). Many of these methods make use of odometer estimates derived from scan matching algorithms such as the method discussed in [7] and the Ceres-based scan matcher used by Google Cartographer [8], and map structures such as occupancy grids [9].

Example, SLAM methods include HectorSLAM, a 2D SLAM method without loop closure that uses a 2D occupancy grid map and a bilinear interpolator to achieve better scan matching performance [11]. More recently, Google introduced Google Cartographer, a 2D and 3D SLAM package with loop closure that uses data from a single and multiple aperture laser range scanner to generate 2D and 3D maps of the environment using probabilistic occupancy grids [12]. Modified 2D laser scanners have been used in [13], [14], and [15] to add a height estimator using measurements from a deflected section of the 2D laser field-of-view (FoV). This concept is expanded in the Lidar Optical Navigation (LION) method proposed in [1] that uses 2 or more laser range scanners installed on the platform to estimate the height-above-ground rather than deflect just a part of one of the lasers. This comes with the benefit that the height estimator also performs correctly in the presence of slanted ground surfaces.

An alternative to laser-based sensors for navigation and mapping purposes is the use of cameras either monocular or stereo. In [16], the authors give an overview of some of the existing Vision Odometry (VO) and Visual Inertial Odometry (VIO) and uses flight data to evaluate various methods using optical flow, extracted features and photometric information from the image pixels. Whereas this paper focusses on the navigation performance of the algorithm, some of the referenced papers and others focus on both pose estimation and map generation (i.e., SLAM). [17] provides a taxonomy of vision-based SLAM techniques, dividing them into **direct** methods that use the photometric information from the image pixels and **indirect** methods that pre-process the image and use extracted features or optical flow vectors to estimate pose and build a map via reconstruction. Furthermore, the paper also categorizes method according the number of points used for pose estimation and reconstruction of the map: **dense** methods that use all of the image points, **sparse** methods that use only a selected set of independent points, and **semi-dense** methods that use a large subset of the points. Examples of indirect, sparse methods are PTAM [18] and the more recent ORB-SLAM [19] and ORB-SLAM2 [20]. LSD-SLAM [21] and DTAM [22] are examples of direct, dense methods. Finally, [17] is an example of a direct, sparse method. Methods such as Semi-Direct Visual Odometry (SVO) [23] are considered hybrid methods as they use both direct and indirect methods.

2. SMALL-SIZE UAS PLATFORM

Before describing the navigation and mapping approach in the next section, this section will address the sUAS platform used. The sUAS platform, shown in Figure 2) consists of a small racing drone platform equipped with an UTM-30LX laser range scanner (~30m range), a RPLIDAR A2M6 laser range scanner (~16m range), a mvBlueFOX-MLC202bG

Monochrome global shutter camera with a 1280x960 resolution, and a PIXRACER flight controller with a built-in low-cost barometric altimeter and inertial measurement unit (IMU). The payload, furthermore, consists of an onboard Odroid XU4 processor running Ubuntu 14.04 and the Robotic Operating System (ROS) version Indigo. In total, the platform plus payload has a weight of 1.3 kg and its dimensions equal 38cm-by-34cm-by-14cm.



Figure 2. Dual laser scanner vision inertial quad-copter racing drone platform.

The orientation of the laser scanners and camera is shown in Figure 3. The two laser scanner orientations are chosen to optimize their ability to perform SLAM in the horizontal direction (x-y plane) and altitude estimation (y-z plane).

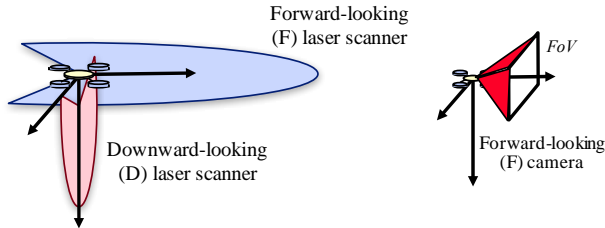


Figure 3. Installation of the two laser scanners and the monochrome camera with respect to the sUAS frame.

3. NAVIGATION METHOD

The overall block diagram of the laser-inertial-optical navigator (LION) is shown in Figure 4. In an environment where GPS is available, the platform can use a GPS/Inertial navigation algorithm. The LION architecture uses the tight GPS/INS integration approach detailed in [24]. This method uses two separate estimators: one for the dynamics (i.e., velocity, and inertial errors sources such as the biases and misorientation) and one for the position. When laser or vision measurements of the environment are available, the bottom two methods will run in parallel and their outputs can be used in addition to GPS to estimate the IMU error

states. However, when GPS is sparse or unavailable, the method will completely rely on available information from the laser range scanners and camera. Both methods to obtain pose and mapping results from laser and vision data are discussed in the next two sections.

3.1 Laser-based Navigation Solution

The center dashed box in Figure 4 shows the laser-based navigation and mapping solution. In this method, the laser range measurements from the forward-looking (FL) laser range scanner, $\mathbf{p}_{i,F,3D}^b$, and the downward-looking (DL) laser range scanner, $\mathbf{p}_{i,D,3D}^b$, are first converted to a locally level using the attitude estimates $(\hat{\phi}, \hat{\theta})$ from the inertial's attitude computer (top box): $\mathbf{p}_{i,F,3D}^l$ and $\mathbf{p}_{i,D,3D}^l$. Next, the DL measurements are used to estimate the altitude and change in altitude of the sUAS above ground level, \hat{h}^n and $\Delta\hat{h}^n$ using the method introduced in [1].

The FL measurements are input to a 2D SLAM algorithm such as *HectorSLAM* or *Cartographer* (both of which are implemented in the setup) to find the 2D location $\hat{\mathbf{r}}_{2D}^n = (x, y)$, the heading ψ , the change in position $\Delta\hat{\mathbf{r}}_{2D}^n$, the change in heading, $\Delta\psi$, and a 2D map, \mathbf{M}_{2D} of the environment represented by an occupancy grid or likelihood field. All these estimates can be combined to obtain an estimate of the 3D pose and 3D pose change:

$$\begin{bmatrix} \mathbf{r}_{LS}^n \\ \boldsymbol{\psi}_{LS} \end{bmatrix} \text{ and } \begin{bmatrix} \Delta\mathbf{r}_{LS}^n \\ \Delta\boldsymbol{\psi}_{LS} \end{bmatrix} \quad (1)$$

where $\boldsymbol{\psi}_{LS}$ is the 3D orientation vector (x, y, ψ) .

Note that the IMU measurements can be input to the SLAM methods as well to improve the solution.

3.2 Vision-based Navigation Solution

Although the real-time results are mostly based on laser range scanner data, some vision-based pose estimation and mapping algorithms were evaluated in post-processing mode as well. The four general approaches discussed in Section 1 are shown in the bottom box in Figure 4. Note that in case of imagery, the problem is formulated as a 3D problem and not broken into an altitude component and a horizontal component as was done with the laser-based solution.

3.3 Error State Estimator

In case no GPS is available, the incremental pose (position and orientation) output by the laser-based navigator or the vision-based navigator can be used to estimate the inertial errors. For more details, the reader is referred to [1].

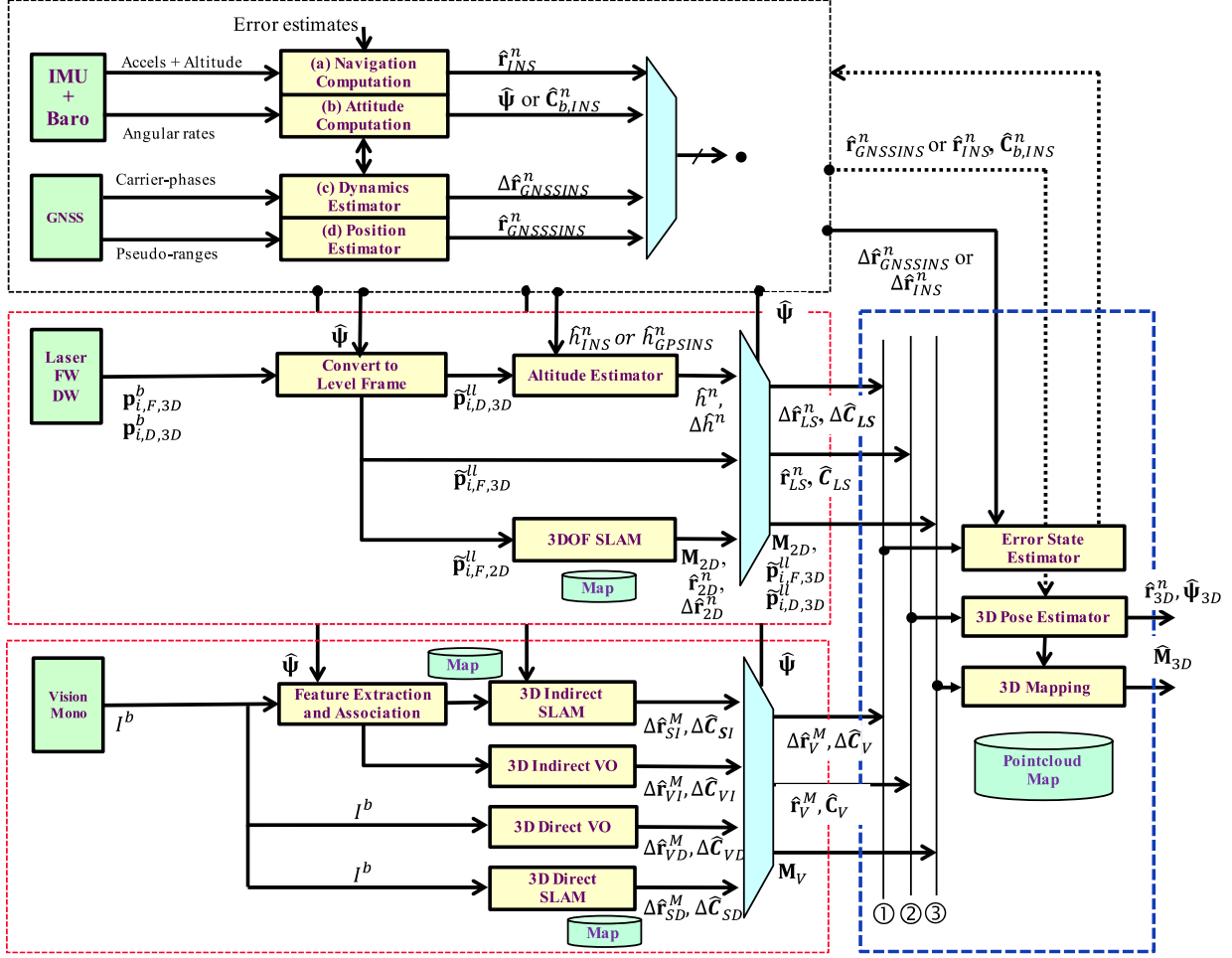


Figure 4. LION High-level functional block diagram of the hierarchical guidance, navigation and control function.

4. MAPPING METHOD

Given the position and orientation (i.e., pose) estimates, $\hat{\mathbf{r}}_{3D}^n$ and $\hat{\mathbf{C}}_b^n$ (based on attitude and heading vector Ψ), obtained in Section 3, the laser range scanning data can be converted to a 3D point-cloud that represents the environment (i.e., map).

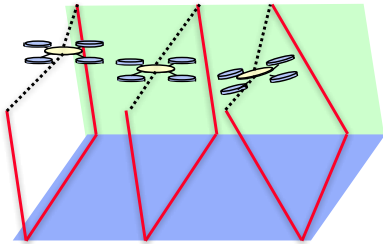


Figure 5. Laser range scans at various points along the trajectory.

This “referencing” process can be described by:

$$\mathbf{p}_{i,X,3D}^n = \hat{\mathbf{r}}_{3D}^n + \hat{\mathbf{C}}_b^n (\mathbf{C}_s^b \mathbf{p}_{i,X,3D}^s + \ell) \quad (2)$$

where X is F for the FL laser range scanner, and D for the DL laser range scanner, ℓ is the lever arm between the platform’s reference point and the sensor reference point, and \mathbf{C}_s^b is coordinate transformation due to the relative orientation of the laser range scanner with respect to the platform’s body axes.

During an earlier test, point cloud data was generated using the LION mapper and compared to truth reference data from a Riegl LMS-Z210 terrestrial mapper. Accuracies of approximately dm-level were obtained for the approximately 4-minute flight through the basement of the Stocker engineering center. Some results of this comparison are shown in Figure 6.

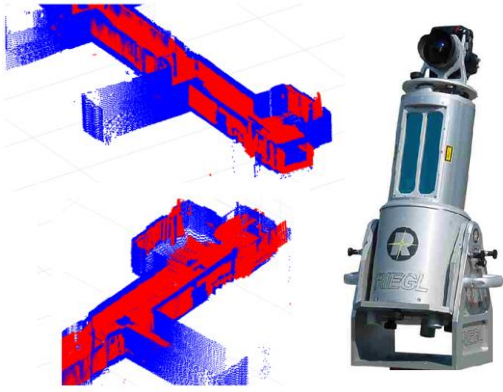


Figure 6. Left: two map examples (blue: Riegl truth reference; red: map based on UAS laser range scanners); Right: Riegl LMS-Z210 terrestrial mapper.

5. VIRTUAL REALITY SOFTWARE MODULE

After the point cloud has been references is transmitted to the ground reference station via WiFi where it is input to the Virtual Reality (VR) software module implemented in Unity. A block diagram of this software is shown in Figure 7.

The software module consists of two threads: the *udpListenerTask* and the *MeshBuilder* object. The former thread waits for a UDP packet to arrive from the sUAS, extracts the points and stores them in a common buffer available to both threads. The *MeshBuilder* checks the contents of the common buffer and, after it contains sufficient points, copies the content of the buffer and uses them to prepare a mesh. Finally, based on this mesh, the thread will create a game object that will be visualized in VR. Note that, at this point, the VR software module

generates a point cloud in VR incrementally. In the future, loop closures in SLAM may require the mesh to be partially or completely be reloaded. Also, future implementation will include additional threads that process the 3D point cloud to extract features such as walls and other objects in the environment.

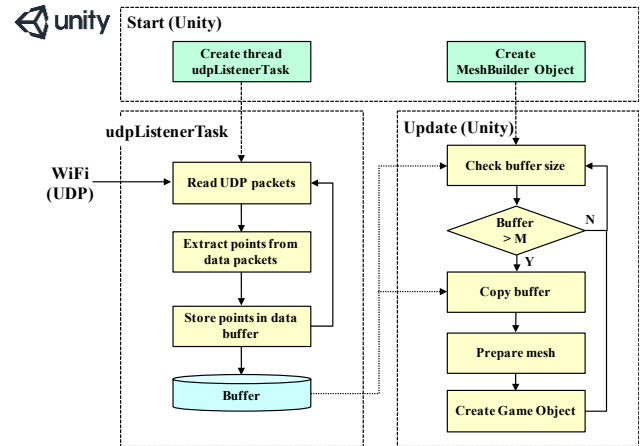


Figure 7. Virtual Reality driver software.

6. INTEGRATED SYSTEM

Figure 8 shows the complete system architecture. The LION and mapping module discussed in sections 3 and 4 interfaces with a module that transmits the point cloud data via WiFi and interacts with the PIXRACER flight controller via a MAVLINK interface. As the software modules onboard the sUAS run under ROS, the MAVROS package is used for this purpose.

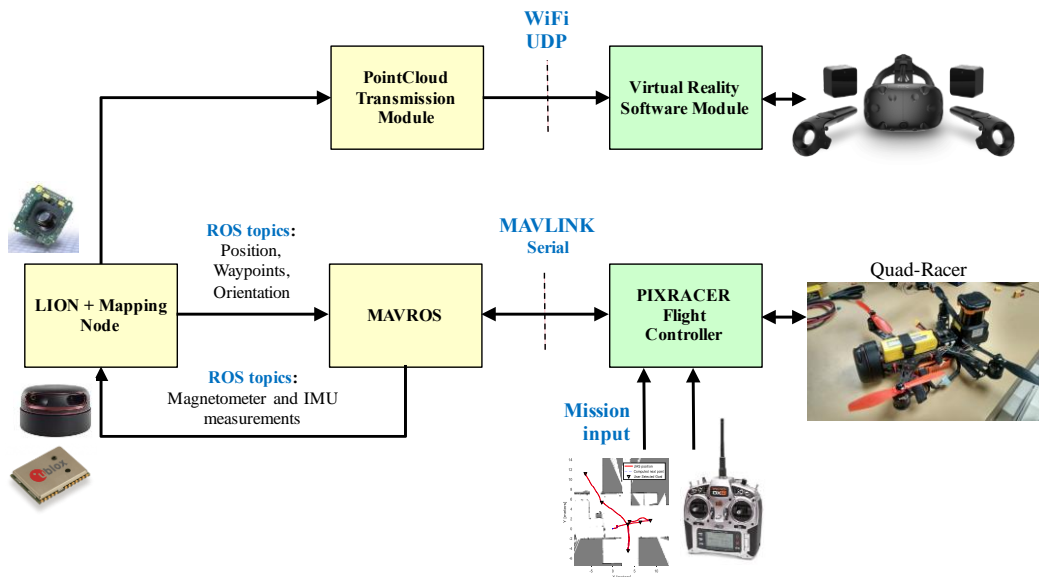


Figure 8. System architecture and interfaces.

The ground station with the VR software module is shown in the top right block. The VR equipment is a HTC Vive.

Various flight modes can be enabled by the FrSky Taranis remote controller:

1. **Manual operation** - user operates multi-copter completely manual;
2. **Altitude hold** – platform maintains current altitude (based on altitude estimate from the LION node), user can change lateral motion.
3. **Position hold** – platform maintains current position (based on position estimate from the LION node), user can change position, but release of the controls causes system to hold at the new position.

4. **Mission mode** – platform follows the flight plan input into the PIXHAWK via software such as QGroundControl.
5. **Offboard mode** – platform follows the waypoint input from the LION node via MAVROS.

More on these modes can be found in [25].

7. FLIGHT-TEST RESULTS

Various flight tests were performed using the real-time mapping sUAS some with VR enabled. This section shows some of the results of these flights. *Figure 9* shows the 3D mapping results for a flight right outside stocker where GPS is only sparsely available.

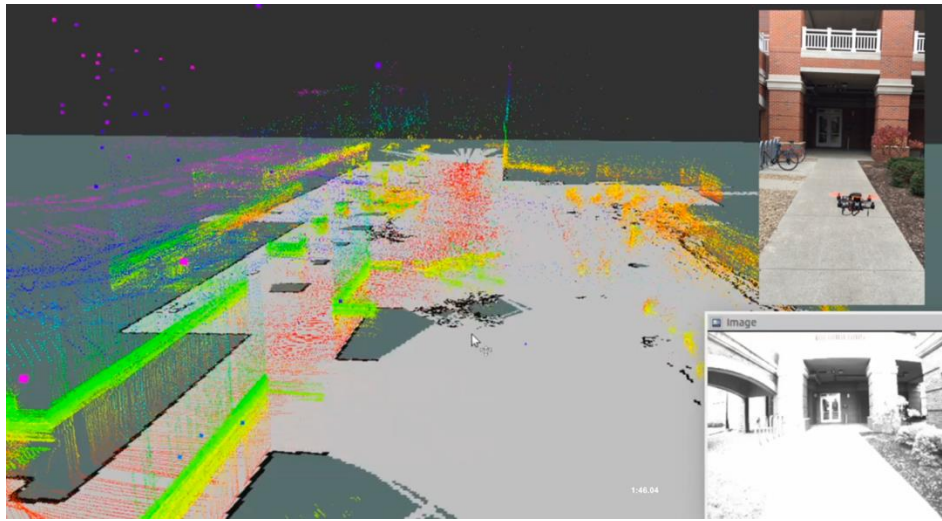


Figure 9. Real-time mapping results using the laser-based navigation and mapping subsystem of LION near Stocker engineering building.

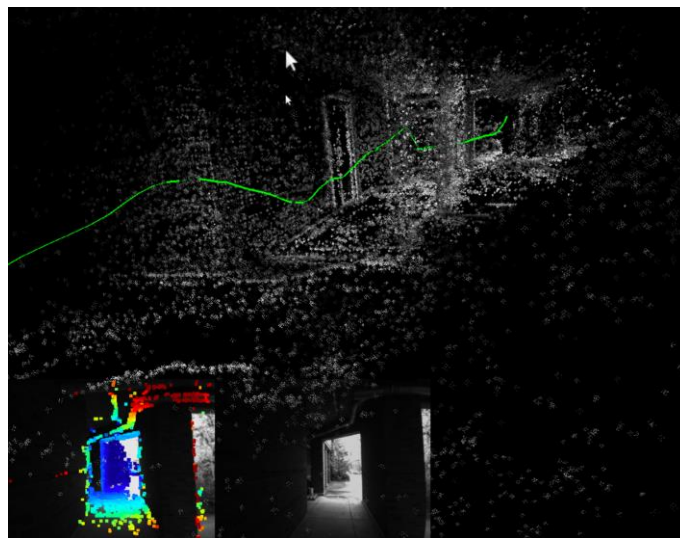
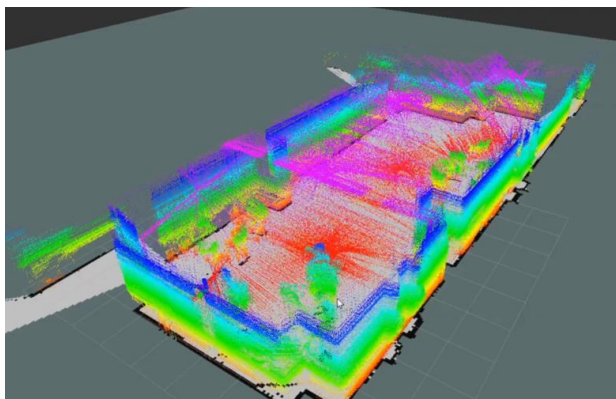


Figure 10. Post-processed mapping excerpt using the visual odometer (DSO) of the vision-based navigation and mapping subsystem of LION near Stocker engineering building.

The referenced scans associated with the horizontal and vertical laser range scanners can be observed clearly superimposed on the 2D occupancy grid provided by the 2D SLAM component of LION. The larger coverage of the horizontal scans in the vertical direction can be attributed to the natural up-and-down motion of the drone under manual operation. This motion can be introduced in the flight plan when operating in the *mission mode*.

Figure 10 shows an example of a map (point cloud) generated with vision-based navigator part of LION using DSO (direct, sparse method) as the visual odometer. One can clearly observe the numerous features within the field of view. Unlike laser-based mapping, the vision-based solution has extent in the horizontal and vertical direction every frame due to its instantaneous field-of-view (FoV).



(a)



(b)

Figure 11. Real-time mapping results using the laser-based navigation and mapping subsystem (a) and VR subsystem output (b) in indoor environment at the Russ Research Center (RRC) in Dayton, Ohio

8. SUMMARY AND FUTURE WORK

This paper described the implementation and demonstration of a small real-time mapping sUAS based on a racing drone platform equipped with two laser range scanners and a monochrome camera. The platform was capable of an approximately 5-minute flight time. Its real-time mapping and VR visualization capability was shown in an indoor and outdoor challenged environment. In addition, the generated data for ~5 mins of flight time were within ~dm of the truth.

Future work will include the real-time generation of a vision-based map and the fusion of vision-based map and laser-based maps, possible using a joint SLAM algorithm. Furthermore, work will include assessment of the integrity of the generated trajectory and map solution and the extension of LION to unstructured environments. Finally, point cloud processing methods will be investigated to improve the visual assessment capability in the ground

The integration of a vision-based map and the laser-based map will therefore be part of future work.

Finally, Figure 11 shows a snapshot of the real-time mapping module of LION (a) and the output of the VR software module as depicted on the HTC Vive (b). In this scenario, the sUAS was operating in an indoor environment inside one of the buildings of the Russ Research Center (RRC) in Dayton, Ohio. Simultaneous, a user was able to observe the growing map in VR on the HTC Vive headset. The sUAS was controlled to perform specific motion to increase the point density of the map such as rotational motion (clearly visible by the star-like laser scan pattern on the left and right in Figure 11) and intentional up-and-down motion.

station including the extraction of walls and man-made objects.

9. ACKNOWLEDGEMENTS

The flight tests were in part funded by the Ohio University Russ Legacy Avionics Engineering Center (AEC) Development Fund.

REFERENCES

- [1]. E. Dill, M. Uijt de Haag, "3D Multi-copter Navigation and Mapping using GPS, Inertial and LiDAR," *NAVIGATION*, Vol. 63, Summer 2016.
- [2]. M. M. Miller, M. Uijt de Haag, A. Soloviev, M. Veth, "Navigating in Difficult Environments: Alternatives to GPS – 1," Proceedings of the NATO RTO Lecture Series on "Low Cost Navigation Sensors and Integration Technology," SET-116, November 2008.

- [3]. M. M. Miller, J. Raquet, M. Uijt de Haag, "Navigating in Difficult Environments: Alternatives to GPS – 2," Proceedings of the NATO RTO Lecture Series on "Low Cost Navigation Sensors and Integration Technology," SET-116, November 2008.
- [4]. A. Soloviev and M. Uijt de Haag, "Three-Dimensional Navigation of Autonomous Vehicles Using Scanning Laser Radars: Concept and Initial Verification," *IEEE Transactions on Aerospace and Electronic Systems*, Vol. 46, Issue 1, 2010.
- [5]. A. Soloviev, M. Uijt de Haag, "Monitoring of Moving Features in Laser Scanner-Based Navigation," *IEEE Transactions on Aerospace and Electronic Systems*, Vol. 46, Issue 4, 2010.
- [6]. M. Uijt de Haag, D. Venable, and M. Smearcheck, "Use of 3D laser radar for navigation of unmanned aerial and ground vehicles in urban and indoor environments," *Proceedings of the SPIE - Volume 6550*, SPIE Defense and Security Symposium, Orlando, FL, April 9- 13, 2007.
- [7]. A. Censi, "An ICP variant using a point-to-line metric" *Proceedings of the IEEE International Conference on Robotics and Automation (ICRA)*, 2008.
- [8]. Google, *Cartographer ROS Documentation*, Release 1.0.0, December 2017.
- [9]. G. Grisetti, C. Stachniss, W. Burgard, "Improving Grid-based SLAM with Rao-Blackwellized Particle Filters by Adaptive Proposals and Selective Resampling," *Proc. Of the IEEE Intl. Conf. on Robot. And Autom.*, Barcelona, Spain, April 2005, pp. 2432-2437.
- [10]. A. Nüchter, *3D Robotic Mapping – The Simultaneous Localization and Mapping Problem with Six Degrees of Freedom*, Springer, 2010.
- [11]. S. Kohlbrecher, O. von Stryk, J. Meyer, U. Klingauf, "A Flexible and Scalable SLAM System with Full 3D Motion Estimates," *Proc. Of IEEE Conference on Safety, Security, and Rescue Robotics*, 2011.
- [12]. W. Hess, D. Kohler, H. Rapp, and D. Andor, Real-Time Loop Closure in 2D LIDAR SLAM, in *IEEE International Conference on Robotics and Automation (ICRA)*, 2016. pp. 1271–1278.
- [13]. S. Shen, N. Michael, V. Kumar, "Autonomous Multi-Floor Indoor Navigation with a Computationally Constrained MAV," *Proc. Of IEEE Conference on Robotics and Automation*, 2011.
- [14]. S. Grzonka, G. Grisetti, W. Burgard, "A Fully Autonomous Indoor Quadrotor," *IEEE Transactions on Robotics*, Vol. 28, Issue 1, 2012.
- [15]. I. Dryanovski, R. G. Valenti, J. Xiao, "An open-source navigation system for micro aerial vehicles," *Autonomous Robotics*, 34, pp177–188, 2013.
- [16]. D. Carson, J. Raquet, K. Kaufmann, "Aerial Visual-Inertial Odometry Performance Evaluation," Proceedings of the 2017 Pacific PNT, Waikiki, HI.
- [17]. J. Engel, V. Koltun, and D. Cremers, "Direct sparse odometry," To appear in *IEEE Transactions on Pattern Analysis and Machine Intelligence*.
- [18]. G. Klein and D. Murray, "Parallel tracking and mapping for small AR workspaces," In *IEEE and ACM Int. Sym. on Mixed and Augmented Reality (ISMAR)*, pp225–234, Nara, Japan, November 2007.
- [19]. R. Mur-Artal, J. M. M. Montiel, and J. D. Tardós. "ORB-SLAM: a versatile and accurate monocular SLAM system," *IEEE Transactions on Robotics*, Vol. 31, No. 5, pp1147–1163, 2015.
- [20]. R. Mur-Artal, and J. D. Tardós, "ORB-SLAM2: an Open-Source SLAM System for Monocular, Stereo and RGB-D Cameras," *IEEE Transactions on Robotics*, Vol. 33, No. 5, Oct. 2017.
- [21]. R. Newcombe, S. Lovegrove, and A. Davison, "DTAM: Dense tracking and mapping in real-time," *In Intl. Conference on Computer Vision (ICCV)*, 2011.
- [22]. J. Engel, J. Schöps, and D. Cremers. LSD-SLAM: Large-scale direct monocular SLAM. *In Eur. Conf. on Computer Vision (ECCV)*, 2014.
- [23]. C. Forster, M. Pizzoli, and D. Scaramuzza, "SVO: Fast semi-direct monocular visual odometry," *Proceedings of the Intl. Conference on Robotics and Automation (ICRA)*, 2014.
- [24]. Farrell, J. L., *GNSS Aided Navigation & Tracking – Inertially Augmented or Autonomous*, American Literary Press, 2007.
- [25]. A. Schultz, R. Gilabert, M. Uijt de Haag, "Indoor Flight Demonstration Results of an Autonomous Multi-copter using Multiple Laser Inertial Navigation," Proceedings of the 2016 International Technical Meeting of the Institute of Navigation, Monterey, CA, January 2016.